Magnetic field fluctuation features at Swarm's altitude: a fractal approach

Paola De Michelis[1], Giuseppe Consolini[2] and Roberta Tozzi[1]

Correspondence to: Paola De Michelis, Istituto Nazionale di Geofisica e Vulcanologia, Via di Vigna Murata 605, 00143 Roma, Italia; Phone: +390651860315; Email: paola.demichelis@ingv.it.

[1]Istituto Nazionale di Geofisica e Vulcanologia, 00143, Roma, Italy.

[2]INAF-Istituto di Astrofisica e Planetologia Spaziali, 00133, Roma, Italy.

The ESA Swarm mission provides a qualitatively new level of observational geomagnetic data, which allows us to study the spatial features of magnetic field fluctuations, capturing their essential characteristics and at the same time establishing a correlation with the dynamics of the systems responsible for the fluctuations. Our study aims to characterize changes in the scaling properties of the geomagnetic field's spatial fluctuations by evaluating the local Hurst exponent, and to construct maps of this index at the Swarm's altitude ($\sim$ 460 km). Since a signal with a larger Hurst exponent is more regular and less erratic than a signal with a smaller one, the maps permit us to localize spatial structures characterized by different scaling properties. This study is an example of the potential of Swarm data to give new insights into ionosphere-magnetosphere coupling; at the same time, it develops new applications where changes in statistical parameters can be used as a local indicator of overall magnetospheric-ionospheric coupling conditions.

1. Introduction

It is well-known that the magnetic field observed at or near the Earth's surface is not constant, but affected by variations on different temporal and spatial scales [*Courtillot and Le Mouël*, 1988].

The magnetic field's temporal variations with periods from seconds to several hundred minutes are the result of processes related to the interaction between the solar wind and the Earth's magnetic field. As a result of this interaction, a considerable amount of energy is released, giving rise to a number of important phenomena in the magnetosphere and upper atmosphere. Examples include large-scale plasma motions, electric currents, aurorae, and disturbances of the neutral and ionized upper atmosphere [*Prölss*, 2006]. Some of these phenomena can be identified readily in magnetograms, recorded both on the ground at geomagnetic observatories and in near-Earth space by satellites orbiting our planet.

Within this system, the European Space Agency's Swarm mission provides a good opportunity for an average study of the magnetic fields of external origin on a global scale. The multipoint measurements of the Swarm constellation mission provide a qualitatively new level of observational data, which allows us for the first time to solve the spatio-temporal features of the magnetic field fluctuations of external origin, to capture their essential characteristics at the Swarm's altitude ($\sim$ 460 km), and, at the same time, to attempt to establish a correlation with the dynamics of the system responsible for such fluctuations. However, some difficulties arise when this type of data is used. The external contributions to the geomagnetic field are ordered primarily in a local time frame;

satellites in a polar orbit, like those of the Swarm constellation, can obtain a reasonably dense sampling of the internal components within a few days, but fails to provide adequate spatial coverage of the external contributions, because of the slow orbital precession through local time. Thus, the Swarm constellation configuration does not allow real-time monitoring of the magnetic field's spatial fluctuations, but only an average study of them.

Recently, the study of magnetic field fluctuations of external origin, recorded both on the ground and in different parts of the Earth's magnetosphere, has been addressed by many researchers because it has permitted a better understanding of the complex magnetospheric dynamics in response to solar wind changes. The analysis of magnetic field fluctuations and in particular of the geomagnetic indices has played a crucial role in several works [*Tsurutani et al.*, 1990; *Consolini et al.*, 1996; *Consolini and Chang*, 2001; *Sharma et al.*, 2001; *Uritsky et al.*, 2002; *Consolini et al.*, 2005, 2008] where the nonlinear properties of the magnetospheric dynamics have been discussed with special attention to the occurrence of chaos, turbulence, and criticality. However, if the analysis of geomagnetic indices permits us to study temporal changes of the magnetic field fluctuations, the measurements of the Swarm constellation provide a unique opportunity to study the spatial features of magnetic field fluctuations at high resolution. The vector field magnetometer (VFM) produces measurements of the field's vector at a sampling rate of 1 Hz which, with a satellite speed of 7.6 km/s, corresponds to a spatial resolution of about 7.6 km along the orbital track.

We use the local Hurst exponent for investigation of the scaling features of geomagnetic field fluctuations at temporal scales below 40 s (corresponding to spatial scales below $\sim$ 300

km) because this quantity, which is a measure of the way in which a data series varies in time, can be used to obtain significant results for the characterization of dynamical systems. The local Hurst exponent can be used to characterize the persistence of a system, e.g., whether the sign of the fluctuations will remain the same (persistent) or change (anti-persistent) from one point to the next, thus providing information on the existence of localized spatial structures. In recent years, there has been increasing interest in the analysis of the Hurst exponent of geomagnetic signals. However, we have found no studies, which analyze satellite data to reconstruct maps of the Hurst exponent to characterize the spatial scaling features of geomagnetic field fluctuations.

The aim of this letter is to investigate the spatial distribution of the local Hurst exponent in high-latitude regions for two different geomagnetic activity levels and to attempt an interpretation in terms of spatial fluctuation structures, and physical processes responsible for them.

2. Dataset Description

The present work focuses on the analysis of the fluctuations of the horizontal component of the Earth's magnetic field from 1st January 2014 to 30th June 2014. These time series have been computed using the calibrated and corrected measurements of the vector magnetic components in the North-East-Center local Cartesian coordinate frame recorded by one of the three satellites of the Swarm constellation (Swarm A) (product of Swarm/VFM and ASM: Swarm level 1b (LR)(MAGA_LR)). The time interval analysed contains both periods of relatively low geomagnetic activity and periods characterised by the occurrence of moderate activity. Being interested in the high-latitude regions (lati-

tude higher than 50° N), we choose the Auroral Electrojet (AE) index to discriminate the different magnetospheric activity levels. The AE index is designed to provide a global, quantitative measure of auroral zone magnetic activity produced by enhanced ionospheric currents flowing below and within the auroral oval. In this work we have selected two different activity levels: AE< 60 nT (quiet geomagnetic activity level) and AE> 80 nT (disturbed geomagnetic activity level) according to the statistical features of AE-index [*Consolini and De Michelis*, 1998]. One-minute data of this index have been downloaded from OMNI data set, where the available data stop at 30$^{\text{th}}$ June 2014, which justified our selection of Swarm's dataset.

3. Method of Analysis

For our investigation of magnetic spatial fluctuation features, we use the Hurst exponent H, a measure of the persistence features of a time series. The value of the Hurst exponent lets us ascertain whether the analyzed time series has an anti-persistent or persistent character. It has been shown that a Hurst exponent value between 0 and 0.5 exists for signals with *anti-persistent character* of fluctuations. This means that a positive (negative) fluctuation will tend to be followed by a negative (positive) one. Conversely, a Hurst exponent value between 0.5 and 1 indicates a *persistent character* of fluctuations, so that a positive (negative) fluctuation will tend to be followed by another positive (negative) one – that is, the signal is trending. The larger the H value is, the stronger the trend. In other words, the underlying spatial structure is governed by a positive feedback mechanism of the fluctuations. Lastly, a Hurst exponent value equal to 0.5 indicates that there is no correlation between the repeated increments. This value also marks the

transition between anti-persistent and persistent behavior in a signal. Thus, physically speaking, investigation of the Hurst exponent may allow detection of localized spatially coherent structures.

Since the geomagnetic field fluctuations do not exhibit a simple global scaling behavior which can be described using a single scaling exponent, it is necessary to introduce a multitude of scaling exponents [*Consolini et al.*, 1996; *Consolini and De Michelis*, 1998; *Wanliss*, 2005]. In many physical systems the scaling features acquire a local character, which can have a dependence on the amplitude of fluctuations for multifractal objects, or a time dependence for multifractional signals. Here, instead of using the standard global Hurst exponent to characterize the properties of these time series, it is better to introduce a local Hurst exponent because the scaling properties of time series under investigations cannot be considered constant. Indeed, it is of extreme importance to correctly quantify the long-range correlations of the geomagnetic time series in order to gain a deep understanding of the complex system dynamics that gives rise to the recorded geomagnetic signal.

In the past many different techniques and methods, based on the analysis of time series features in the real or Fourier space, have been proposed to estimate the local Hurst exponent of a time series [*Holschneider*, 1988; *Bacry et al.*, 1993; *Muzy et al.*, 1994; *Peng et al.*, 1992, 1995; *Abry et al.*, 2000; *Alessio et al.*, 2002]. In this paper, we employ an alternative method based on the detrended 1st-order structure function $S_1(\tau)$, which for a signal $x(t)$ defined over an interval T is given by

$$S_1(\tau) = \langle \mid x(t+\tau) - x(t) \mid \rangle_T, \tag{1}$$

where τ is a time separation, and $\langle ... \rangle_T$ indicates time averaging over the interval T. This 1$^{\text{st}}$-order structure function exhibits a power law behavior as a function of the time separation τ when we deal with a scale invariant signal $x(t)$, so that $S_1(\tau) \sim \tau^H$ where H is the Hurst exponent. Thus, the analysis of the scaling features of the 1$^{\text{st}}$-order structure function exponent provides an efficient method for characterizing the correlative structure of a signal as an empirical approximation to the Hurst exponent.

The method used in our analysis can be summarized as follows. Given a time series $y(t)$, we consider a time interval $[t_0 - T/2, t_0 + T/2]$, where T is at least 10 times larger than the maximum scale τ which we want to investigate. In the selected time interval, we detrend the time series by computing the average long-term trend using a 7$^{\text{th}}$-order polynomial fit $p(t)$. In this way, we can construct a new detrended time series $x(t)$,

$$x(t) = y(t) - p(t), \qquad \forall t \in [t_0 - T/2, t_0 + T/2], \tag{2}$$

to which we apply the structure function analysis. We call the complete procedure as *detrended structure function analysis* (DSFA).

In the case of Swarm's data, we have calculated the local Hurst exponent H for fluctuations in the range from 1 s to 40 s, by considering a moving window of 400 s (i.e., $T = 400$ s in our case). The choice of a maximum timescale of 40 s is motivated by the requirements to get local spatial information on the magnetic field fluctuations. Indeed, using the Swarm's satellite velocity and assuming that the evolution time of spatial structures

is longer than the transit time, these temporal scales roughly correspond to investigation of spatial fluctuations from 7.6 km up to $\sim$ 300 km and relate to fluctuations in the magnetohydrodynamic (MHD) domain: the ion-gyroperiod is $T_\Omega = 1/\Omega_i \ll 1$ s, and both the ion-inertial length η_i and the ion-Larmor radius r_L are smaller (much smaller) than 7.6 km for the typical ionospheric plasma parameters at Swarm's altitude ($\sim$ 460 km).

Typical relative error in the estimation of the local Hurst exponent is 4% with a 95% confidence. This error has been evaluated using a Monte Carlo simulation. Figure 1 shows an example of the behavior of the 1$^{\text{st}}$-order structure function $S_1(\tau)$. A clear power law dependence is recovered at the scales investigated here, thus assessing the scale invariance of the analyses signal in the considered range of timescales.

4. Results and Discussion

As described in the previous section, we employ DSFA analysis to determine the statistical nature of our signal. An example of our results is shown in Figure 2, where the computed local Hurst exponent values are plotted for one Swarm A orbit and reported with the corresponding values of AE-index, horizontal component of the geomagnetic field and satellite's geomagnetic latitude. As shown in Figure 2, the character of the analyzed time series is the result of a superposition of structures (set of fluctuations) characterized by different values of the local Hurst exponent in the interval $[0, 1]$. Consequently, during the selected period the analyzed time series are characterized at scales below 40 seconds, both by fluctuations that tend to induce stability within the system, and by fluctuations with a persistent behavior implying a system dynamics governed by a positive feedback mechanism. This sample is chosen to better assess the potential of the local Hurst expo-

nent to delineate and characterize transitions in magnetograms due to dynamical changes of the scaling fluctuation features on spatio-temporal scales.

Figure 3 shows polar view maps of the local Hurst exponent values over the polar region in the northern hemisphere for different geomagnetic activity levels. In the top panel of Figure 3, the spatial distribution of the local Hurst exponent values is reported for the quiet geomagnetic activity level (AE $<$ 60 nT), while the bottom panel shows the same quantity during disturbed intervals (AE $>$ 80 nT). The magnetic field fluctuations with a persistent character are shown in blue, and those with an anti-persistent character in red. As can be seen from the image in Figure 3 (on the top) there is a strong asymmetry in the daily character of the magnetic field fluctuations during the geomagnetic quiet level. At mid/high geomagnetic latitude between 50° N and $\sim$ 70° N magnetic field fluctuations show an anti-persistent character in the sunlit hemisphere ($03 < MLT < 19$) and a mostly persistent one in the dark sector. This difference in magnetic field fluctuation character reflects the morphology and dynamics of that part of the ionosphere which is crossed by the satellite. This region can, to varying degrees, be influenced by solar EUV radiation, energetic particle precipitation, diffusion, thermospheric winds, electrodynamic drifts, polar wind escape, and so on, which have a different behavior in the dark and sunlit hemisphere. Moreover, the high-latitude ionosphere differs significantly from its mid-latitude counterpart because, given the geometry of the geomagnetic field, which is to a first approximation dipolar, the high-latitude ionosphere is more directly modified by magnetospheric processes that are largely controlled by the interaction between the solar

wind and the Earth's magnetosphere. In fact, many ionospheric phenomena that occur at high latitudes are footprint signatures of this interaction.

During the quiet periods, the different dynamics of the magnetic field fluctuations seem to describe physically different areas in the polar regions. The white profile, which delimits the spatial transition from an anti-persistent to a persistent dynamics, roughly corresponds to the boundary of the northern magnetic auroral oval. The spatial extension of this region changes with the geomagnetic activity level. In the bottom map of Figure 3, the local Hurst exponent values are reported for the disturbed geomagnetic activity level. The strong asymmetry in the daily character of the magnetic field's spatial fluctuations is still evident, but the region of anti-persistent character becomes smaller ($05 < MLT < 17$) than in the previous case, and the position of the white profile shifts towards geomagnetic latitude values less than 70° N in average, while the persistent region shows an increasing equatorward extent in the dark sector.

5. Summary and Conclusions

The time series of the geomagnetic field's horizontal component recorded by the Swarm A satellite were statistically analyzed in terms of scaling (fractal) features. The local Hurst exponent of the horizontal component was used to describe the spatio-temporal persistence character of the magnetic field fluctuations at high latitudes in the northern hemisphere during quiet and disturbed geomagnetic activity levels.

Maps of the local Hurst exponent give us the opportunity to localize the different latitudinal structures caused by different physical processes. The regions characterized by a larger value of the H exponent display magnetic field fluctuations with a larger spatio-

temporal coherence than the regions with a smaller H. Assuming that the observed fluctuations concern spatial fluctuations (i.e., under Taylor's hypothesis of frozen-in advected structures), because for a scale-invariant (fractal) signal there is a direct relationship between the Hurst exponent H and the exponent β of the power spectral density ($S(k) \sim k^{-\beta}$ where $\beta = 2H + 1$ and k is the wavenumber), we can suggest that the ionospheric polar regions characterized by different H values have different behaviors of the spectral density $S(k)$ with the wavenumber k. Consequently, the geomagnetic field's spectral density is characterized by $\beta > 2$ ($\beta \sim 2.5 - 2.6$) in those regions where the Hurst exponent assumes values greater than $\frac{1}{2}$ (for instance in the polar cap and auroral oval), while the spectral exponent is $\beta < 2$ ($\beta \sim 1.6 - 1.8$) in those regions with H values smaller than $\frac{1}{2}$ (such as in the dayside of high and mid latitude regions).

This interpretation is partially supported by similar spectral regimes in the long-wavelength domain observed analyzing the turbulence properties of the electric field fluctuations at various altitudes over the auroral zone and polar cap [*Weimer et al.*, 1985; *Heppner et al.*, 1993; *Golovchanskaya et al.*, 2006; *Kozelov et al.*, 2008] where substantial differences between the scaling features of the fluctuations are not found in the two regions, as in our case [*Golovchanskaya et al.*, 2010]. However, there is not a simple correlation between the electric and magnetic fields, so that the results obtained for the electric field cannot be straight forwardly considered valid for the magnetic field. *Sugiura et al.* [1982] demonstrated a remarkably good correlation between the north-south component of the electric field (E_x) and the east-west component of the magnetic field (B_y) and *Weimer et al.* [1985] revealed that the Fourier spectra of these two components exhibited similar

power laws. Anyway, there is not a general one-to-one correspondence between the electric field E_x and magnetic one B_y, being this correspondence valid only in the auroral oval, where the magnetic field lines are closed [*Smiddy et al.*, 1980; *Golovchanskaya et al.*, 2006]. Moreover, the present analysis treats the horizontal component of the geomagnetic field and not of the single B_y component, and it describes an average result obtained using about 3000 crossings without diversifying into different interplanetary magnetic field conditions. Thus, our findings seem to be consistent with those by other authors suggesting that the scaling properties of the magnetic field fluctuations in the auroral oval and in the polar cap are basically the same. In contrast to earlier findings, however, our results suggest that in these regions magnetic field fluctuations are characterized by power law spectra with exponents $\beta > 2$ at all the scales analyzed. Indeed, *Golovchanskaya et al.* [2006, 2010] found that the power spectra of the electric field exhibit power-law relations characterized by a break at scale ~ 40 km, such that the slope β of the spectrum is greater ($\beta > 2$) for scales smaller than 40 km and lower ($\beta < 2$) for scales over 40 km.

The different character of the spectral features that we find analyzing the magnetic field fluctuations in the high-latitude polar regions may be a consequence of distinct turbulent regimes: *i*) a strong shear-flow turbulence regime with $\beta \sim 3$ (as in the polar cap and auroral oval); *ii*) a shear-flow turbulence with an inverse energy cascade and/or a strong gradient drift or current convective turbulence, which are both characterized by a spectral index $\beta \sim 5/3$ (as in the dayside high-latitude regions). In this picture, because for the disturbed activity level we observe an expansion of the region characterized by a Hurst exponent $H > 1/2$, this could be a consequence of plasma transport increase from distant

equatorial magnetotail regions during magnetic substorms, causing an expansion of the region affected by strong shear flow turbulence due to an enhancement of plasma convection. We remark that the emergence of turbulence must be related to the enhancement of plasma density irregularities and Kelvin-Helmholtz instability.

In conclusion, this study shows the potential of ESA's Swarm mission to reveal the physical character of ionospheric high-latitude turbulence and its dependence on the geomagnetic activity level.

Acknowledgments. The results presented in this paper rely on data collected by the Swarm A satellite. We thank the European Space Agency that supports this mission. The authors kindly acknowledge N. Papitashvili and J. King at the National Space Science Data Center of the Goddard Space Flight Center for the use permission of 1-min OMNI data and the NASA CDAWeb team for making these data available. Giuseppe Consolini acknowledges funding from the European Community's Seventh Framework Programme ([FP7/2007-2013]) under Grant no. 313038/STORM. The elaborated data for this paper are available by contacting the corresponding author.

References

Abry P., P. Flandrin, M.S. Taqqu, and D. Veitch (2000), Wavelets for the analysis, estimation and synthesis of scaling data, in *Self-similar Network Traffic and Performance Evaluation*, edit by K. Park and W. Willinger, p. 39, Wiley-Interscience, Hoboken, N.J.

Alessio E., A. Carbone, G. Castellli , and V. Frappietro (2002), Second-order moving average and scaling of stochastic time series, *Eur. Phys. J.*, *B 27*, 197-200.

Bacry, E., J. F. Muzy, and Arnéodo (1993), A. Singularity spectrum of fractal signals from wavelet analysis: Exact results. *J. Stat. Phys.*, *70*, 635674.

Consolini G., M. F. Marcucci, and M. Candidi (1996), Multifractal structure of auroral electroject index data, *Phys. Rev. Lett.*, *76*, 4082.

Consolini G., and P. De Michelis (1998), Non-Gaussian distribution function of AE-index fluctuations: evidence for time intermittency, *Geophys. Res. Lett.*, *25*, 4087.

Consolini G., and T. Chang (2001), Magnetic field topology and criticality in geotail dynamics: relevance to substorm phenomena, *Space Sci. Rev.*, *95*, 309.

Consolini G., T. Chang, and A. T. Y. Lui (2005), Complexity and topological disorder in the Earth's magnetotail dynamics, in *Nonlinear transitions in plasma*, Sharma A. S. and P. Kam (eds.), Kluwer.

Consolini G., P. De Michelis, and R. Tozzi (2008), On the Earth's magnetospheric dynamics: nonequilibrium evolution and the fluctuation theorem, *J. Geophys. Res.*, *113*, A8, doi:10.1029/2008JA013074.

Courtillot V., and J. L. Le Mouël (1988), Time variations of the Earth's magnetic field, *Ann. Rev. Earth Planet. Sci.*, *16*, 389-476.

Golovchanskaya, I.W., A.A. Ostapenko and B.V. Kozelov, (2006), Relationship between the high-latitude electric and magnetic turbulence and the Birkeland field-aligned currents, *J. Geophys. Res.*, *111*, A12301, doi: 10.1029/2006JA0111835.

Golovchanskaya, I.W. and B.V. Kozelov, (2010), On the origin of electric turbulence in the polar cap ionosphere. *J. Geophys. Res.*, *115*, A09321, doi: 10.1029/2009JA014632.

Heppner, J.P., M.C. Liebrecht, N.C. Maynard and R.F. Pfaff (1993), High-latitude distributions of plasma waves and spatial irregularities from DE2 alternating current field electric field observations. *J. Geophys. Res.*, *98*, 1629-1652.

Holschneider, M. (1988), On the wavelet transformation of fractal objects. *J. Stat. Phys.*, *50*, 963-993.

Kozelov, B.V., Golovchanskaya, I.W., A.A. Ostapenko and Y.V, Federenko (2008), Wavelet analysis of high latitude electric and magnetic fluctuations observed by Dynamic Explorer 2 satellite, *J. Geophys. Res.*, *113*, A03308, doi: 10.1029/2007JA012575.

Muzy, J. F., E. Bacry, and A. Arnéodo (1994), The multifractal formalism revisited with wavelets. *Int. J. Bifurcat. Chaos*, *4*, 245-302.

Peng, C.-K. et al. (1992), Long-range correlations in nucleotide sequences, *Nature*, *356*, 168.

Peng, C.-K. et al. (1995), Mosaic organization of DNA nucleotides, *Phys. Rev. E*, *49*, 1685.

Prölss, G.W. (2006), *Physics of the Earth's Space Environment: An Introduction*, Springer.

Sharma A. S., M. I. Sitnov, and K. Papadopoulos (2001), Substorms as nonequilibrium transitions of the magnetosphere, *J. Atmos. Sol. Terr. Phys.*, *63*, 1399.

Smiddy, M., W.J. Burke, N.A. Saflekos, M.S. Gussenhoven, D.A. Hardy and F.J. Rich., (1980), Effects of high-latitude conductivity on observed convection electric fields and Birkeland currents, *J. Geophys. Res.*, *85*, 6811-6818.

Sugiura, M., N.C. Maynard, W.H. Farthing, J.P. Heppner, B.G. Ledley and L.J. Cahill Jr., (1982), Initial results on the correlation between the magnetic and electric fields observed from DE 2 satellite, *Geophys. Res. Lett.*, *9*, 985-988.

Tsurutani B. et al. (1990), The nonlinear response of AE to the IMF Bs, *Geophys. Res. Lett.*, *17*, 279.

Uritsky V. M., A. J. Klimas, D. Vassiliadis, D. Chua, and G. D. Parks (2002), Scale free statistics of spatiotemporal auroral emissions as depicted by POLAR UVI images: The dynamic magnetosphere is an avalanching system, *J. Geophys. Res.*, *107*, 1426.

Wanliss J. A. (2005), Fractal properties of SYM-H during quiet and active times, *J. Geophys. Res.*, *110*, doi:10.1029/2004JA010544.

Weimer D.R., C.K. Goertz, and D.A. Gurnett (1985), Auroral zone electric fields from DE1 and 2 at magnetic conjunctions, *J. Geophys. Res.*, *90*, 7479-7494.

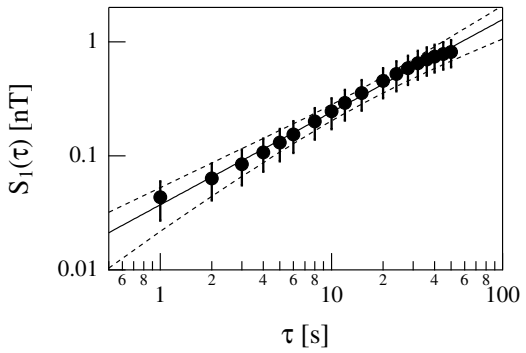

Figure 1. A sample of the behavior of the 1st order structure function $S_1(\tau)$. The solid line is a power-law fit. Dashed lines show the 95% confidence interval.

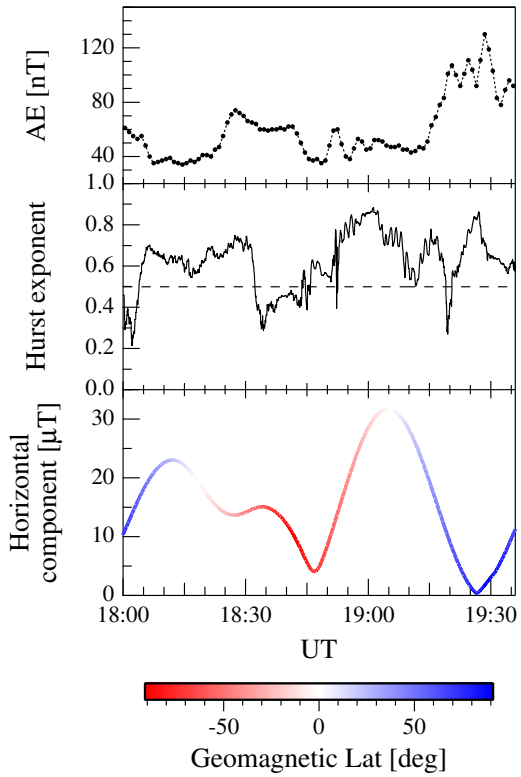

Figure 2. From top to bottom: the Auroral Electrojet (AE) index, the local Hurst exponent (H) and the magnetic field horizontal component for an orbit of the Swarm A satellite on April 1st, 2014. Dashed horizontal line (intermediate panel) is for $H = 0.5$ and the color scale reported in the bottom plot shows the geomagnetic latitude of Swarm A during the selected orbit.

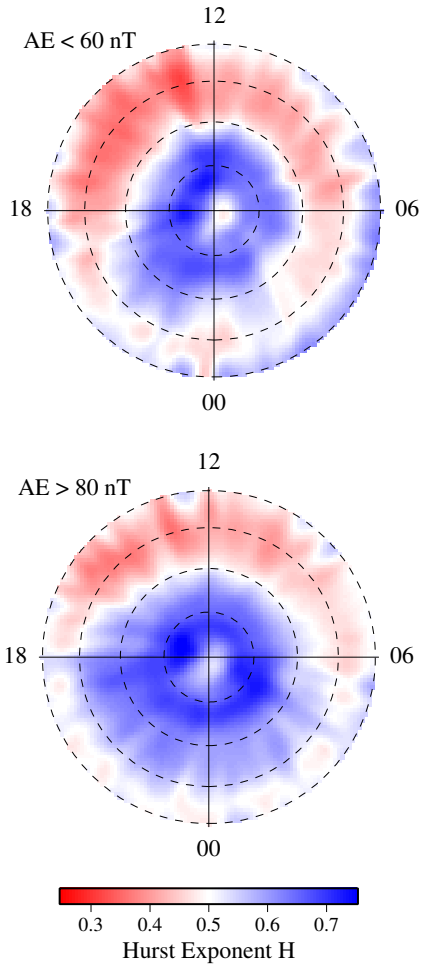

Figure 3. The local average Hurst exponent values in the northern hemisphere in a polar representation of magnetic local time (MLT) and geomagnetic latitude. Top and bottom maps refer to quiet (AE $<$ 60 nT) and disturbed (AE $>$ 80 nT) periods, respectively. Dashed circles are located at geomagnetic latitudes of 50° N, 60° N, 70° N and 80° N.